X-ray diffraction study of WO_3 at high pressure

2002 J. Phys.: Condens. Matter 14 6605

(http://iopscience.iop.org/0953-8984/14/26/301)

INSTITUTE OF PHYSICS PUBLISHING JOURNAL OF PHYSICS: CONDENSED MATTER

J. Phys.: Condens. Matter **14** (2002) 6605–6617 PII: S0953-8984(02)30266-2

X-ray diffraction study of WO_3 at high pressure

P Bouvier[1,2], W A Crichton[1], M Boulova[2,3] and G Lucazeau[2]

[1] ESRF, BP220, 38043 Grenoble Cedex, France
[2] Laboratoire d'Electrochimie et de Physico-Chimie des Matériaux et des Interfaces UMR 5631 CNRS-INPG, 1130 rue de la Piscine, BP75, 38402 St Martin d'Hères, France
[3] Chemistry Department, Moscow State University, Moscow, 119899, Russia

Received 26 October 2001, in final form 8 May 2002
Published 21 June 2002
Online at stacks.iop.org/JPhysCM/14/6605

Abstract

The high-pressure behaviour of microcrystalline tungsten oxide (WO_3) has been investigated with angle-dispersive synchrotron x-ray powder diffraction in a diamond anvil cell up to 40 GPa at room temperature. Up to 21 GPa, the pressure dependence of the volume of the monoclinic high-pressure ($P2_1/c$) phase is described by a third-order Birch–Murnaghan equation of state with parameters $V_0 = 210.9(7)$ Å^3, $K_T = 27(2)$ GPa and $K' = 9.4(5)$. At 24 GPa, a first-order phase transition occurs with an approximate ΔV of 7.4% to a monoclinic $P2_1/a$ unit cell with $a = 6.1669(8)$ Å, $b = 4.5758(6)$ Å, $c = 5.3159(6)$ Å, $\beta = 101.440(9)°$. A second transition is observed at pressures higher than 31 GPa with an approximate ΔV of 12% to a phase described by a third monoclinic unit cell, with $a = 10.3633(22)$ Å, $b = 3.9065(8)$ Å, $c = 9.3459(18)$ Å and $\beta = 98.539(14)°$.

1. Introduction

Tungsten trioxide, WO_3, is subject of intensive research because of its great applicability in electrochromic devices, catalysis or as a precursor for hard-materials synthesis [1–3]. At room temperature, the triclinic δ-phase ($P\bar{1}$, $V_0 = 422.5$ Å^3, $Z = 8$ [4]) is considered to be thermodynamically stable although it often coexists with other phases such as the monoclinic γ-phase ($P2_1/n$, $V_0 = 423.7$ Å^3, $Z = 8$ [4–6]).

Literature on high-pressure investigations of the WO_3 phase transition is scarce. In their early high-pressure study, Salje and Hoppmann [7] observed that the initial mixture of γ- and δ-phases undergoes a partial transformation into the δ-phase under modest pressure, and then, on further pressure increase, completely into the *monoclinic* ε-phase (P_c, $V_0 = 208.5$ Å^3, $Z = 4$) at 0.15 GPa. This phase is similar to the low-temperature phase [8, 9]. An x-ray diffraction study of single-crystal WO_3 performed up to 5.7 GPa allowed Xu *et al* [10] to conclude that the triclinic form is transformed into a new monoclinic phase ($P2_1/c$, $V_0 = 211$ Å^3, $Z = 4$), distinct from the ε-phase reported by Salje and Hoppmann, above 0.57 GPa. More recently, the Raman data obtained by Souza-Filho *et al* [11] have shown that the complete transformation

takes place above 1.4 GPa, without putting forward any spectroscopic arguments for deciding between the P_c or $P2_1/c$ space groups.

Only recently, pseudopotential *ab initio* calculations have indicated the $P2_1/c$ space group as an optimized structure for the high-pressure phase of WO_3 [12]. These calculations have shown that upon compression the shape and size of the WO_6 octahedron units, which are the building blocks of these perovskite-like structures, are hardly affected by volume change. The crystal responds to pressure only by a rotation of neighbouring octahedra. The calculated energy versus volume curve is flat and the bulk modulus obtained from the Birch equation of state (EoS) is low. This result is in agreement with the low value of the bulk modulus (44.5 GPa) obtained by Xu *et al* [10] from their diamond anvil cell (DAC) experiment.

The present study is complementary to a recent Raman high-pressure study [13] in which spectral anomalies have been observed near 3 and 10 GPa while a new high-pressure phase was obtained at 22 GPa. This latter transition was characterized by a marked spectral change and is most likely of first order, whereas the spectral anomalies were associated with small structural changes. Note that if these spectral changes involve large displacements of atoms in general positions, they do not necessarily involve a change of space group or of cell multiplicity. Here we investigate the high-pressure room temperature behaviour of the WO_3 compound with angle-dispersive x-ray powder diffraction in a DAC. We pay special attention to the phase transitions. The bulk modulus and cell anisotropy of the compound are measured.

2. Experimental details

Tungsten oxide powder of 99.995% purity was obtained from Aldrich. The initial phase composition was deduced from x-ray diffraction and found to be a mixture of monoclinic γ- and triclinic δ-structures in an approximate 90:10 ratio. The average crystallite size is 0.5 μm.

High-pressure synchrotron x-ray diffraction experiments were performed at the European Synchrotron Radiation Facility (ESRF) on the ID30 beamline. The sample was loaded in a DAC with diamond tips of diameter 350 μm. Nitrogen was used as the pressure-transmitting medium in order to maintain good hydrostatic conditions. The pressure was measured using the ruby fluorescence method [14] with a precision of 0.02 GPa below 20 GPa. X-ray diffraction patterns were collected in an angle-resolved geometry on an image plate detector (Mar345) with a focused monochromatic beam at wavelength $\lambda = 0.3738(1)$ Å. The sample-to-detector distance and the image plate inclination angles were precisely calibrated using a silicon standard [15]. The two-dimensional diffraction images were analysed using the ESRF Fit2D software [16], yielding intensity versus 2θ patterns.

The data were analysed by profile matching (Le Bail) and by full Rietveld refinements using FULLPROF [17] software. The refined parameters are the scale factor, Chebyshev polynomial background, lattice parameters (a, b, c and β), fractional coordinates and isotropic thermal parameters. The peak shapes were described with a pseudo-Voigt function. The profile parameters u, v, w, lx, ly, which determine the resolution function (see the FULLPROF manual), were obtained from the refinement of a high-purity silicon standard. Preferred orientation parameters were not refined. Bragg reflections from the solid phases of the nitrogen [18] pressure-transmitting medium were excluded from the refinements.

3. Results

X-ray diffraction patterns were recorded up to 40 GPa with small pressure increments. Some typical patterns recorded between 3.4 and 19.9 GPa are shown in figure 1. The patterns

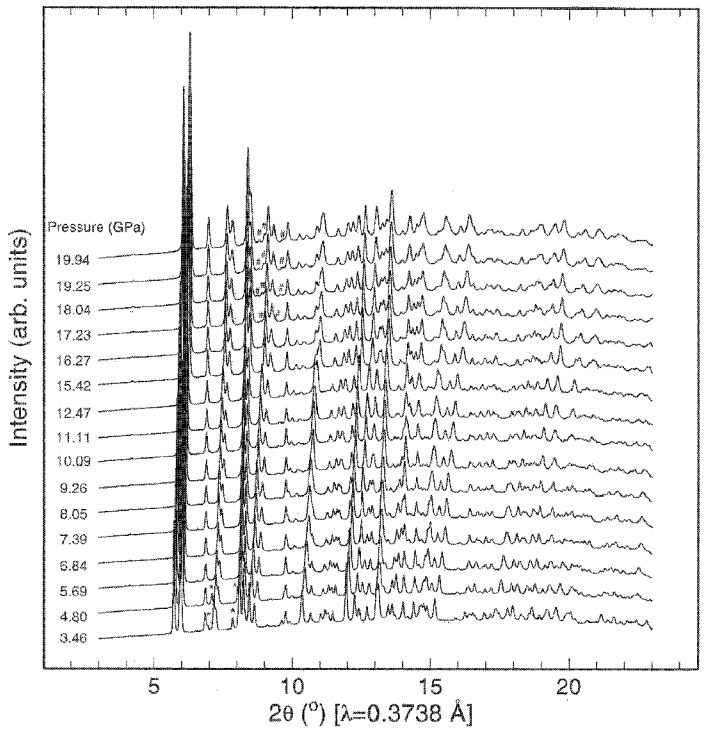

Figure 1. Pressure evolution of the x-ray diffraction pattern of WO_3. The pressure is indicated on the left side of each pattern. Markers indicate the lines of the nitrogen β-phase ($P6_3/mmc$) and ε-phase ($R\bar{3}c$) of the pressure-transmitting medium.

recorded for pressures higher than 20 GPa are shown in figure 2. Markers in both figures indicate the lines of the nitrogen β-phase ($P6_3/mmc$) and ε-phase ($R\bar{3}c$). Up to 20.8 GPa, the patterns are characteristic of the $P2_1/c$ structure already reported by Xu *et al* [10] and there is no indication of any major structural transformation, whereas at 21.8 GPa, the change observed within a pressure range of 3 GPa (21.8–24.9 GPa) is an indication that a new high-pressure polymorph of WO_3 is formed. At higher pressure (>31.9 GPa), the pattern evolved further (see the inset in figure 2), especially at low angle. We will show that the compound undergoes a second phase transition. During decompression, we observed that the initial pattern is recovered for pressure lower than 15 GPa.

3.1. Unit-cell volume and equation of state for $P < 20\ GPa$

Below 20.87 GPa, the patterns were refined in the monoclinic $P2_1/c$ space group. The unit-cell parameters measured at 1.06 GPa in the DAC are found to be equal to $a = 5.2557(3)$ Å, $b = 5.0986(3)$ Å, $c = 7.6242(3)$ Å and $\beta = 92.169(4)°$, in good agreement with the Xu *et al* [10] single-crystal values, i.e. $a = 5.253(3)$ Å, $b = 5.100(1)$ Å, $c = 7.641(7)$ Å and $\beta = 92.30(6)°$ at 0.99 GPa.

The pressure evolution of the unit-cell volume is reported in figure 3. Unit-cell parameters are given in table 1. The data obtained by Xu *et al* [10] are shown for comparison. The parameters obtained by fitting the P–V data between 1.06 and 20.87 GPa with a third-order Birch–Murnaghan [19] EoS are $V_0 = 210.9(7)$ Å^3, $K_T = 27(2)$ GPa and $K' = 9.4(5)$. These

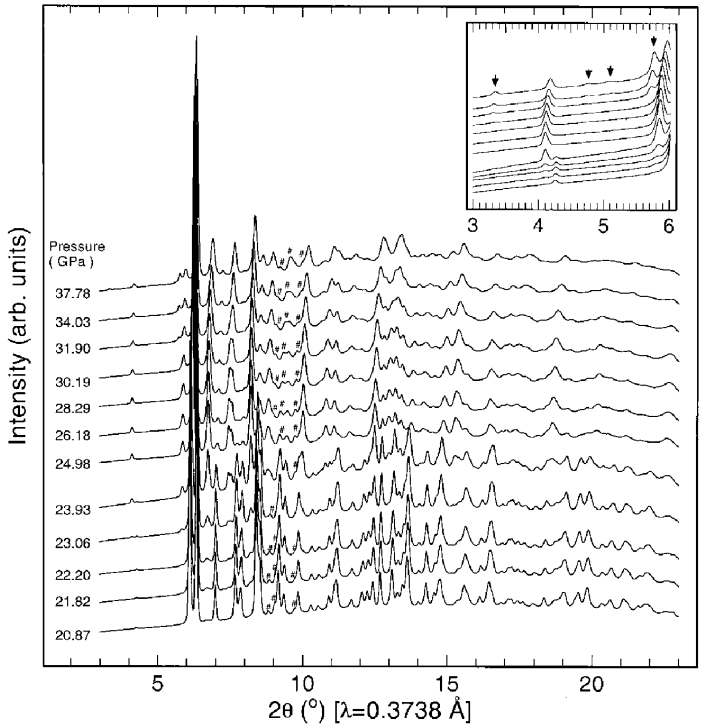

Figure 2. Pressure evolution of the x-ray diffraction pattern for pressure higher than 20 GPa. The pressure is indicated on the left side of each pattern. Markers indicate the lines of nitrogen ε-phase ($R\bar{3}c$) of the pressure-transmitting medium. The phase transition toward a new high-pressure polymorph of WO_3 is clearly seen from the change of the pattern at 21.82 GPa. The inset gives an enlargement of the high-pressure patterns in the low-2θ region. The observation of new peaks, which are pointed to by arrows, show that a second phase transition is taking place above 31.9 GPa.

values fall to $V_0 = 207.8(4)$ Å^3, $K_T = 45(1)$ GPa when fixing K' to 2.5 and keeping the pressure below 6 GPa, indicating the equivalence of the Xu *et al* data with these results.

The compression data are plotted as Birch's normalized pressure, $F = P/[3f(1+2f)^{5/2}]$, against the Eulerian strain measure, $f = (1/2)[(V/V_0)^{-2/3} - 1]$ (see e.g. [20]), in figure 4. The $F-f$ plots provide a visual indication that of whether higher-order terms are significant in the EoS. The fact that the present data (plotted for V_0 fixed at 210.9 Å^3) lie on an inclined straight line means that the data are correctly described by a third-order Birch–Murnaghan EoS.

3.2. Phase transition for $P > 22$ GPa

At 21.8 GPa, the observation of weak new reflections in the diffraction pattern shows that a new high-pressure polymorph of WO_3 is formed. The observation of a large pressure buffering with two-phase coexistence is probably related to kinetic effects and/or to strong first-order nature of the transition. For this reason, the pattern recorded at 26.18 GPa was chosen to be representative of the new pattern. The 2θ peak positions were obtained for peaks $>2\% I/I_{max}$. The positions were indexed by DICVOL91 [21], giving $M(20) = 29.1$, $F(20) = 124.1(0.0034, 48)$ for a monoclinic unit cell with $a = 6.1598(21)$ Å, $b = 4.5705(21)$ Å, $c = 5.3156(14)$ Å and $\beta = 101.412(16)°$.

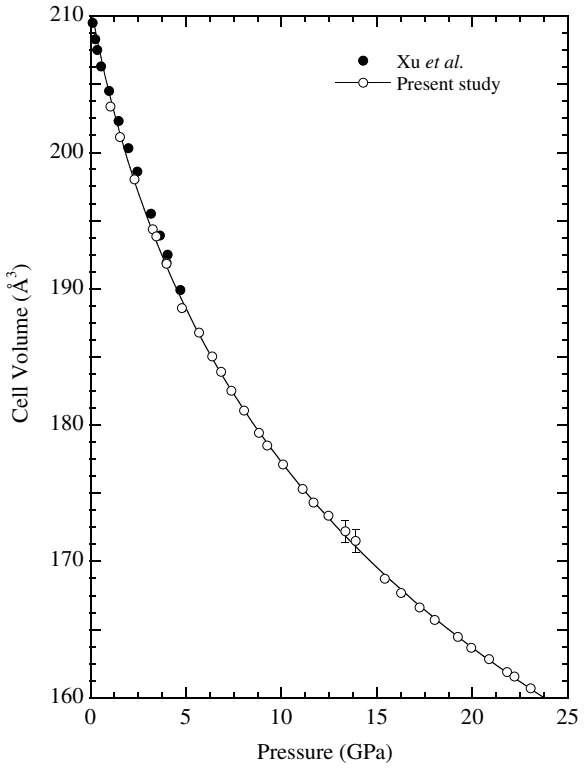

Figure 3. Unit-cell volume evolution with pressure obtained from Le Bail refinement in the monoclinic $P2_1/c$ space group. The full circles correspond to data obtained by Xu *et al* [10] from single-crystal x-ray diffraction. The open circles correspond to the present work. The parameters extracted from the third-order Birch–Murnaghan EoS (plain line) are equal to $V_0 = 210.9(7)$ Å^3, $K_T = 27(2)$ GPa and $K' = 9.4(5)$.

The pressure evolution of the unit-cell volume obtained from Le Bail least-squares refinement of patterns between 21.82 and 30.19 GPa is reported in figure 5. Experimental values are given in table 3. The volume variation upon transition is found equal to $\Delta V_{24\,\mathrm{GPa}} = 11.90$ Å^3, $\Delta V/V = 7.4\%$. The compression parameters can be measured from least-squares refinement of the volume variation $K_T = -V_0\,\mathrm{d}P/\mathrm{d}V$ and are found equal to $V_0 = 148.1(1)$ Å^3, $K_T = 296(2)$ GPa at 24 GPa. The phase transition involves a strong increase of bulk modulus, because the present value is much larger than the value (253 GPa) extrapolated at this pressure in the previous phase.

A density of 10–10.5 g cm^{-3} is expected through estimation of the compressibility of WO_3 up to the transition pressure. Thus the number of formula units is expected to be four, as in the previous structure. Analysis of systematic absence allowed the space groups $P2$, $P2_1$, Pm, $P2/m$, $P2_1/m$ and $P2_1/a$ to be proposed. However, the space group $P2_1/a$, which corresponds to the maximum checked reflection and the minimum calculated reflections, can be considered as the best space group. This choice is further supported by the fact that the Raman spectra did not show any augmentation in the total number of lines upon transition. We attempted to obtain a model for use in Rietveld refinement using 2θ–I data and the indexed monoclinic cell using the ENDEAVOUR program [22, 23]. We choose the lowest-R structure for automated symmetry element and translation search, giving again a unique space group of $P2_1/a$. Preliminary Rietveld refinement of the tungsten sublattice could then be performed

Table 1. Unit-cell parameters obtained from Le Bail refinements in the $P2_1/c$ monoclinic space group as a function of pressure. The numbers in brackets indicate the error in the last significant figure.

P (GPa)	a (Å)	b (Å)	c (Å)	β (deg)	V (Å^3)
1.06(1)	5.2557(3)	5.0986(3)	7.6242(3)	92.169(4)	204.16(2)
1.56(1)	5.2460(4)	5.0696(4)	7.5993(5)	92.442(6)	201.92(2)
2.31(1)	5.2336(5)	5.0288(5)	7.5633(6)	92.826(7)	198.81(2)
3.27(1)	5.2191(6)	4.9809(6)	7.5193(7)	93.280(8)	195.15(2)
3.99(1)	5.2097(5)	4.9486(5)	7.4895(7)	93.586(8)	192.71(2)
3.46(1)	5.2132(3)	4.9652(3)	7.5019(6)	93.424(3)	193.83(2)
4.00(1)	5.2047(4)	4.9396(4)	7.4763(5)	93.662(3)	191.82(2)
4.80(1)	5.1863(4)	4.9026(4)	7.4343(6)	93.951(4)	188.58(3)
5.69(1)	5.1846(3)	4.8741(3)	7.4121(5)	94.320(3)	186.77(2)
6.38(1)	5.1777(4)	4.8516(3)	7.3894(5)	94.555(3)	185.04(3)
6.84(2)	5.1729(4)	4.8368(4)	7.3748(5)	94.704(3)	183.90(3)
7.39(1)	5.1669(4)	4.8191(4)	7.3567(6)	94.881(3)	182.52(3)
8.05(2)	5.1604(4)	4.8005(4)	7.3376(6)	95.064(3)	181.06(3)
8.83(1)	5.1530(4)	4.7800(4)	7.3155(6)	95.281(3)	179.43(3)
9.26(2)	5.1502(4)	4.7694(4)	7.3049(6)	95.401(3)	178.50(3)
10.09(2)	5.1426(4)	4.7499(4)	7.2836(6)	95.597(3)	177.12(3)
11.11(2)	5.1341(4)	4.7279(4)	7.2592(6)	95.814(4)	175.30(3)
11.69(3)	5.1293(4)	4.7154(4)	7.2455(6)	95.918(4)	174.31(3)
12.47(4)	5.1257(4)	4.7025(4)	7.2318(6)	96.055(4)	173.34(4)
13.36(1)	5.1213(5)	4.6873(5)	7.2159(7)	96.201(5)	172.21(4)
13.90(3)	5.1182(5)	4.6780(5)	7.2061(7)	96.292(5)	171.50(4)
15.42(1)	5.0973(5)	4.6490(5)	7.1663(7)	96.531(5)	168.72(4)
16.27(1)	5.0917(5)	4.6365(5)	7.1510(7)	96.660(5)	167.68(4)
17.23(2)	5.0866(5)	4.6235(5)	7.1348(7)	96.793(5)	166.62(4)
18.04(4)	5.0818(5)	4.6125(5)	7.1206(7)	96.896(6)	165.70(5)
19.25(3)	5.0752(5)	4.5979(5)	7.1005(7)	97.017(6)	164.45(5)
19.94(2)	5.0699(6)	4.5898(6)	7.0879(7)	97.088(6)	163.67(6)
20.87(2)	5.0656(6)	4.5799(6)	7.0736(7)	97.177(6)	162.82(6)
21.82(1)	5.0595(7)	4.5703(7)	7.0575(9)	97.262(8)	161.88(7)
22.20(3)	5.0575(7)	4.5672(7)	7.0512(9)	97.305(8)	161.55(7)
23.06(3)	5.0519(7)	4.5622(7)	7.0303(9)	97.389(8)	160.69(7)

using FULLPROF. Final convergence was reached with $R_p = 20.3$, $R_{wp} = 18.8$, $\chi^2 = 6$ for tungsten atoms in the 4e Wyckoff position at (0.161, 0.339, 0.231).

3.3. Phase transition for $P > 31$ GPa

For pressure higher than 31 GPa, the diffraction pattern showed further evolution through the observation of several new lines at 2θ equal to 3.34°, 4.76°, 5.10°, 5.77° (figure 2). This shows that the primitive unit-cell volume has changed and that a second phase transition is taking place. 2θ positions were obtained for peaks $>2\% I/I_{max}$ for the pattern recorded at 37.78 GPa and were indexed by DICVOL91 [21]. Again the best unit cell was monoclinic with $a = 10.386(25)$ Å, $b = 3.873(6)$ Å, $c = 9.427(15)$ Å, $\beta = 98.4(1)°$, $V_0 = 375.1$ Å^3, $M(20) = 5.7$, $F(20) = 24.4(0.0111, 74)$.

The phase transition takes place through a multiplication of the unit cell by a factor of three. The pressure evolution of the volume ($(1/3)V_0$) obtained from Le Bail least-squares refinement of the patterns between 31.90 and 37.78 GPa is reported in figure 5. The values are given in

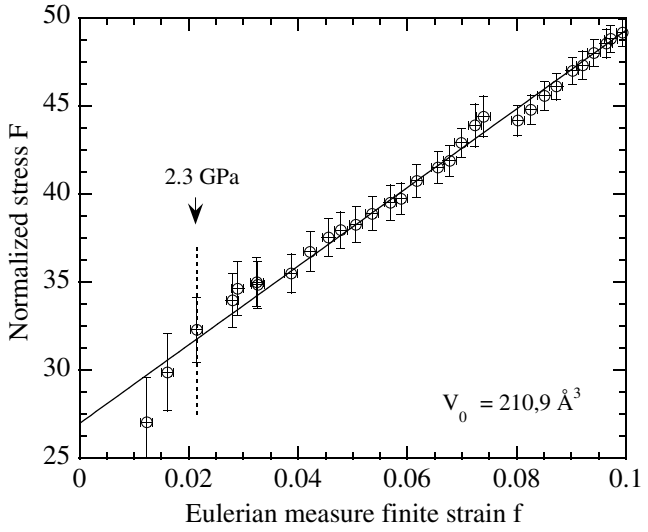

Figure 4. Hydrostatic compression data plotted as Birch's [19] normalized pressure, $F = P/[3f(1+2f)^{5/2}]$, as a function of the Eulerian strain measure $f = (1/2)[(V/V_0)^{-2/3} - 1]$. The value for V_0 is fixed at 210.9 Å from Birch–Murnaghan EoS refinement. The arrow indicates 2.3 GPa.

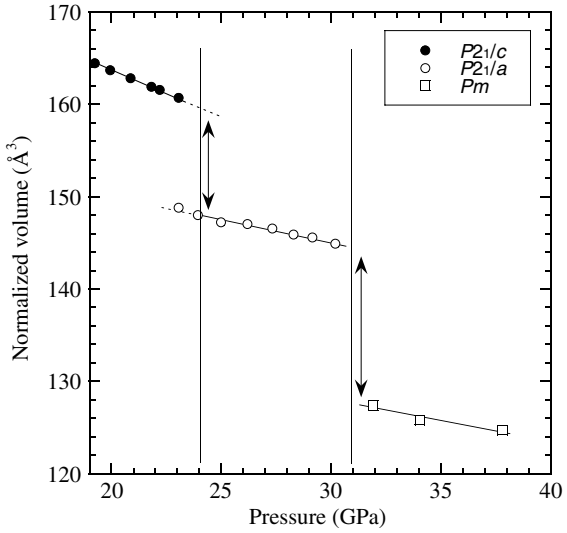

Figure 5. Unit-cell volume evolution with pressure obtained from Le Bail refinement in different monoclinic unit cells. The changes in volume are indicated by arrows.

table 3. The volume variation upon transition is found to be equal to $\Delta V_{31\,\mathrm{GPa}} = 17.4$ Å^3 with $\Delta V/V = 12\%$. The compression parameters obtained from least-squares refinement of the rescaled volume versus pressure curve (see figure 5) are $V_0 = 127.5(5)$ Å^3, $K_T = 350(50)$ GPa at 31 GPa.

Table 2. Peak positions (2θ) measured for the patterns recorded at 26.18 GPa and indexation in the monoclinic $P2_1/a$ space group.

26.18 GPa—$P2_1/a$			
Index	2θ, calculated	2θ, experimental	Intensity
0 0 1	4.1114	4.109	373.8
1 1 0	5.8730	5.873	901.3
0 1 1	6.2323	6.237	16 691
−1 1 1	6.7553	6.758	3 554.3
2 0 0	7.0911	7.094	388.4
−2 0 1	7.4592	7.464	1 614.4
1 1 1	7.5644	7.569	1 368.0
0 0 2	8.2281	8.227	4 042.0
2 1 0	8.5006	8.517	1 377.0
−2 1 1	8.8103	8.823	1 300.4
2 0 1	8.8786		
0 2 0	9.3715		
0 1 2	9.4709	9.478	393.3
−1 1 2	9.5237		
−2 0 2	9.7429	9.747	466.0
1 2 0	10.0220	10.037	2 119.4
2 1 1	10.0418		
0 2 1	10.2374		
−1 2 1	10.5650		
1 1 2	10.6739		
−2 1 2	10.8143	10.829	987.3
1 2 1	11.1015	11.110	871.9
−3 1 1	11.6158		
3 1 0	11.6347	11.644	444.5
2 2 0	11.7616		
2 0 2	11.8922		
−2 2 1	11.9881		
0 0 3	12.3555		
0 2 2	12.4832		
−1 2 2	12.5235	12.529	2 096.9
2 1 2	12.7867	12.793	975.3
2 2 1	12.9231		
−2 0 3	12.9746		
−3 1 2	12.9824	13.000	1 297.4
3 1 1	13.0331		
−1 1 3	13.0357		
0 1 3	13.2193	13.218	1 387.3
1 2 2	13.4219	13.434	936.0

4. Discussion

The present study allows us to confirm that the initial mixture of triclinic and monoclinic forms which are observed for WO_3 at ambient conditions are totally transformed into monoclinic high-pressure phase ($P2_1/c$, $V_0 = 211$ Å^3, $Z = 4$) for $P < 1$ GPa. This result confirms the previous observations [7, 10, 11, 13].

The high-pressure monoclinic phase ($P2_1/c$) is shown to be stable over a wide pressure range (1–23 GPa). The bulk modulus and its derivative, $K_T = 27(2)$ GPa, $K' = 9.4(5)$, are found to be different from the previous published values, $K_T = 44.5(9)$ GPa, $K' = 2.5(4)$ [10].

Table 3. Unit-cell parameters obtained from Le Bail least-squares refinements in $P2_1/a$ (23.06–30.19 GPa) and Pm (31.90–37.78 GPa) monoclinic space groups as a function of pressure. The numbers in brackets indicate the error in the last significant figure.

P (GPa)	a (Å)	b (Å)	c (Å)	β (deg)	V (Å^3)
23.06(3)	6.1731(9)	4.6139(8)	5.3362(8)	101.776(10)	148.79(7)
23.93(3)	6.1704(9)	4.5961(7)	5.3277(8)	101.624(10)	147.99(7)
24.98(3)	6.1686(9)	4.5801(7)	5.3167(7)	101.465(9)	147.22(4)
26.18(3)	6.1669(8)	4.5758(6)	5.3159(6)	101.440(9)	147.03(4)
27.32(2)	6.1607(9)	4.5693(8)	5.3106(8)	101.392(9)	146.55(5)
28.29(4)	6.1581(8)	4.5554(8)	5.3033(7)	101.295(9)	145.89(5)
29.14(3)	6.1534(8)	4.5531(8)	5.2988(7)	101.280(9)	145.59(5)
30.19(3)	6.1328(8)	4.5515(6)	5.2946(6)	101.335(9)	144.91(4)
31.90(3)	10.4399(10)	3.9572(8)	9.3820(24)	99.392(23)	382.40(13)
34.03(9)	10.3908(10)	3.9413(6)	9.3463(17)	99.546(22)	377.46(09)
37.78(2)	10.3633(22)	3.9065(8)	9.3459(18)	98.539(14)	374.17(13)

These differences are due to the fact that, in the previous study, the pressure range was limited to 5 GPa. We have shown that the bulk modulus is strongly increased when fixing K' equal to 2.5 and restricting the pressure range to up to 6 GPa. Moreover, considering the substantial softness of WO_3, we should add that the high value for K' is more realistic. Soft materials are generally associated with high K'-values.

The structural changes, which were deduced from Raman anomalies near 3 and 10 GPa, are not confirmed by similar discontinuities of cell volume or lattice parameters. To gain more insight into more subtle structural features, such as octahedra orientations, we have used full Rietveld refinement. The starting positional parameters for the atoms were those reported in [10]. The results are reported in figure 6, for two different pressures, 3.4 and 9.2 GPa. The pressure dependences of the axial and planar WO bond lengths inside each octahedron are shown in figure 7 up to 14 GPa. The refinement of the patterns recorded for pressure higher than 14 GPa gave unrealistic WO distances and will not be considered further here. This is probably due to larger preferential orientation lowering the ability to resolve oxygen positions. As pressure is increased, the shortest axial bond decreased while the largest one increased, so they reach similar lengths around 8 GPa. This phenomenon is also observed for planar bonds. Thus under pressure, we observed some reorganization of tungsten atoms inside each octahedron without any strong modification of the octahedron volume. Indeed, these observations can explain the spectral anomalies (band softening and splitting) which were observed from Raman experiment. The octahedra are relatively hard and the reduction of the cell volume is governed by progressive tilting and torsion of neighbouring octahedra (see the representations along a- and c-directions in figure 8). The same results were predicted from recent *ab initio* calculations [12].

Similar observations have been reported for rhenium oxide under low pressure [24, 25]. For example, the distorted structures, $P4/mbm$ for $P > 0.5$ GPa and $Im\bar{3}$ for $P > 0.7$ GPa, are known to present small bulk modulus (i.e. 35 GPa). This was explained by considering that high compression can be achieved by coupled rotation around (100) and (111) directions of the parent cubic ($Pm\bar{3}m$) structure, leaving the octahedron undistorted [24]. In fact, ReO_3 and WO_3 belong to the same family of perovskite-like structures (ABO_3) where the central cation A is missing, which enables large rotations of octahedra to occur (see also the discussion in [26]).

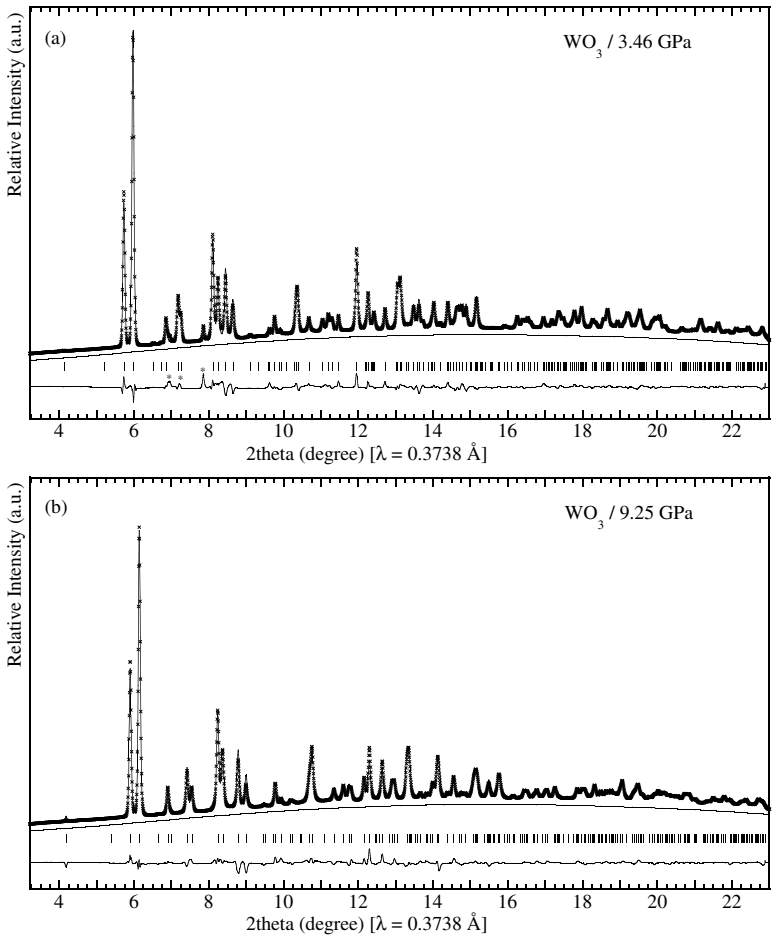

Figure 6. Results of full Rietveld refinements of the x-ray diffraction patterns of WO_3 collected at (a) 3.46 GPa and (b) 9.25 GPa. The refinement is based on a monoclinic $P2_1/c$, $Z = 4$ high-pressure structure with W and O atoms in the 4e general position (x, y, z). The observed, calculated and difference curves are represented. The tick marks indicate the calculated Bragg reflections. The goodness of the refinements is described by the conventional Rietveld R-factors, $R_p = 11.3$, $R_{wp} = 11.4$, ($R_{exp} = 6.95$), $\chi^2 = 2.68$ and $R_p = 11.8$, $R_{wp} = 11.3$, ($R_{exp} = 7.22$), $\chi^2 = 2.43$ for patterns (a) and (b) respectively. Stars indicate the lines of nitrogen β-phase ($P6_3/mmc$) of the pressure-transmitting medium.

4.1. Structure of the new high-pressure phases of WO_3

The present study of the pressure-induced phase transition in WO_3 has revealed the existence of two novel monoclinic phases between 24 and 40 GPa. The sequence of phase transitions with increasing pressure can be described as follows:

$$P\bar{1}, Z = 8 \underset{1\,\mathrm{GPa}}{\rightarrow} P2_1/c, Z = 4 \underset{24\,\mathrm{GPa}}{\rightarrow} P2_1/a, Z = 4 \underset{31\,\mathrm{GPa}}{\rightarrow} \text{monoclinic}.$$

The transition at 24 GPa is strongly first order and involves a strong reduction of the unit-cell volume (7.4%). The full determination of the new structure could not be achieved; however, the space group $P2_1/a$ and the cell parameters were determined. The space group is in agreement with the observation of the same number of Raman bands in both low- and high-pressure

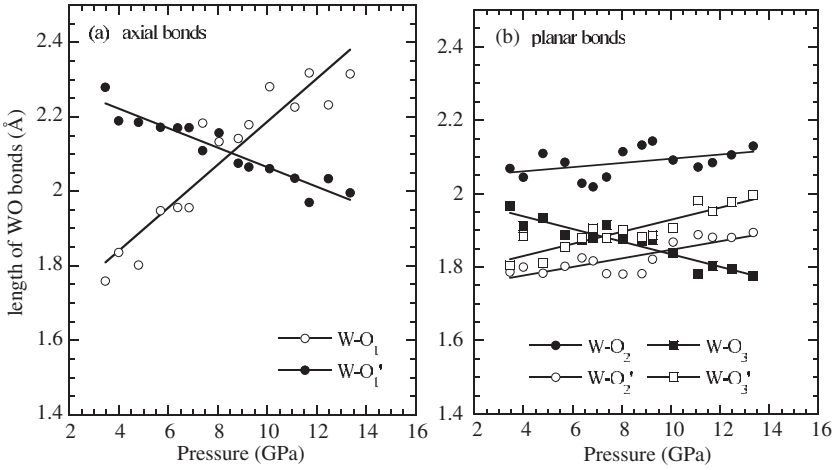

Figure 7. Evolution with pressure of planar and axial WO bonds inside octahedra obtained from full Rietveld refinement between 3 and 14 GPa. The corresponding bonds, i.e. the planar WO_1 and the axial WO_2 or WO_3, are marked in figure 8.

structures [13]. The cell is different from the MnF_3-type structure ($C2/c$ with $a = 8.904$, $b = 5.037$, $c = 13.440$ Å, $\beta = 92.74$, $Z = 12$) which is suggested to be the high-pressure structure of ReO_3 between 3 and 12 GPa on the basis of energy-dispersive x-ray diffraction [25]. The structure is hardly compressible ($K_T = 290$ GPa) compared to the monoclinic MnF_3-type (96 GPa) or the rhombohedral VF_3-type ($R\bar{3}c$, $a = 5.170$ Å, $c = 13.400$ Å, $K_T = 129$ GPa) structures of ReO_3 [25]. The low compressibility of the high-pressure phase is probably related to the compression of octahedra themselves through WO bonds in order to enable volume reduction under pressure.

The transition at 31 GPa is again of first order and implies a multiplication of the unit cell. Again the cell is different from MnF_3- and VF_3-type structures. The bulk modulus ($K_T = 350$ GPa) is of the same order of magnitude as that of the high-pressure polymorph of RuO_3 ($Pa\bar{3}$, i.e. 399 GPa) [27] which corresponds to the hardest oxide known. However, we have shown that, contrary to what is generally observed for these hard oxides, WO_3 cannot be retained down to ambient condition without transforming into the initial cell.

5. Conclusions

The high-pressure behaviour of microcrystalline tungsten oxide has been investigated with synchrotron angle-dispersive x-ray powder diffraction in a DAC up to 40 GPa at room temperature. The results show that the compound exhibits several phase transitions from the already reported monoclinic high-pressure phase ($P2_1/c$, $Z = 4$) to two different monoclinic cells. Both transitions are strongly first order and are located near 24 and 31 GPa. A $P2_1/a$ space group is proposed for the monoclinic cell at 24 GPa. The structural transitions suggested by anomalous variations of Raman parameters are not evidenced by x-ray diffraction.

The pressure dependence of the volume of the monoclinic ($P2_1/c$, $Z = 4$) phase is described by a third-order Birch–Murnaghan EoS. The parameters are $V_0 = 210.9(7)$ Å^3, $K_T = 27(2)$ GPa and $K' = 9.4(5)$. The parameters for the two high-pressure polymorphs are $V_0 = 148.1(1)$ Å^3, $K_T = 296(2)$ GPa at 24 GPa and $V_0 = 127.5(5)$ Å^3, $K_T = 350(50)$ GPa at 31 GPa.

3.4 GPa

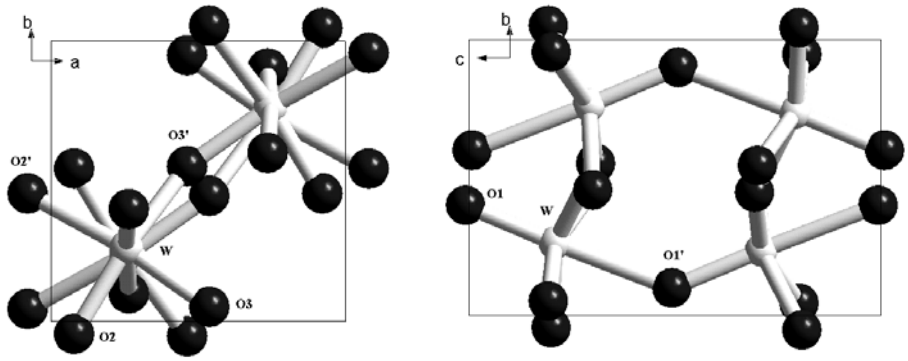

8.0 GPa

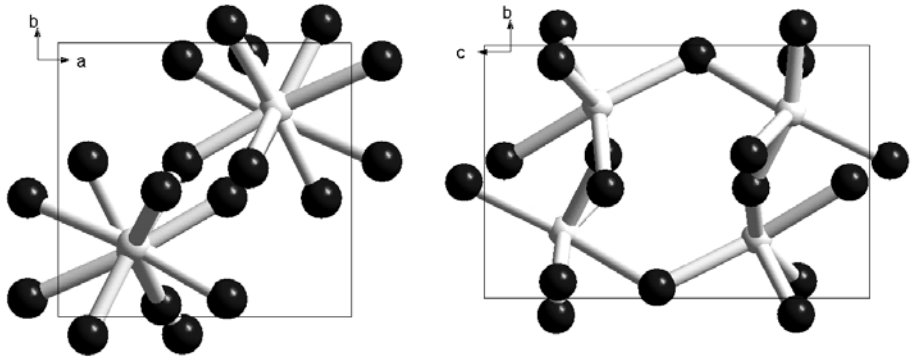

Figure 8. Representations of the tungsten oxygen linkages along *c*- and *a*-directions in the monoclinic $P2_1/c$ structure at 3.4 and 8.0 GPa. The white circles represent tungsten and the dark circles represent oxygen.

References

[1] Granqvist C 1994 *Sol. Energy Mater. Sol. Cells* **32** 369
[2] Aird A, Domeneghetti M, Mazzi F, Tazzoli V and Salje E 1998 *J. Phys.: Condens. Matter* **10** 569
[3] Aird A and Salje E 1998 *J. Phys.: Condens. Matter* **10** 377
[4] Woodward P M, Sleight A W and Vogt T 1995 *J. Phys. Chem. Solids* **56** 1305
[5] Loopstra B O and Boldrini P 1966 *Acta Crystallogr.* B **21** 158
[6] Loopstra B O and Rietveld H M 1969 *Acta Crystallogr.* B **25** 1420
[7] Salje E and Hoppmann G 1980 *High Temp.–High Pressures* **12** 213
[8] Woodward P M, Sleight A W and Vogt T 1997 *J. Solid State Chem.* **131** 9
[9] Salje E K H, Rehmann S, Pobell F, Morris D, Knight K S, Herrmannsdorfer T and Dove M T 1997 *J. Phys.: Condens. Matter* **9** 6563
[10] Xu Y, Carlson S and Norrestam R 1997 *J. Solid State Chem.* **132** 123
[11] Souza-Filho A G, Freire V N, Pilla O, Ayala A P, Filho J M, Melo F E A, Freire V N and Lemos V 2000 *Phys. Rev.* B **62** 3699
[12] Wijs G A D, Boer P K D, Groot R A D and Kresse G 1999 *Phys. Rev.* B **59** 2684
[13] Boulova M, Rosman N, Bouvier P and Lucazeau G 2001 *J. Phys.: Condens. Matter* submitted

[14] Mao H K, Xu J and Bell P M 1986 *J. Geophys. Res.* **91** 4673
[15] Hammersley A P, Svensson S O, Thompson A, Graafsma H, Kvick Å and Moy J-P 1995 *Rev. Sci. Instrum.* **66** 2729
[16] Hammersley A 1995 *ESRF Internal Report* EXP/AH/95-01, FIT2D V5.18 Ref Manual
[17] Rodriguez-Carvajal J 1993 *Physica* B **192** 55
[18] Olijnyk J 1990 *Chem. Phys.* **93** 8968
[19] Birch F 1978 *J. Geophys. Res.* **83** 1257
Birch F 1974 *Phys. Rev.* **71** 809
[20] Jeanloz R and Hazen R M 1991 *Am. Mineral.* **76** 1765
[21] Boultif A and Louer D 1991 *J. Appl. Crystallogr.* **24** 987
[22] Putz H, Schön J C and Jansen M 1999 *J. Appl. Crystallogr.* **32** 864
[23] Bonn 2001 Crystal Impact GbR, Endeavour 1.1, http://www.crystalimpact.com/endeavour, E-mail: infocrystalimpact.com
[24] Jorgensen J-E, Jorgensen J D, Batlogg B, Remeika J P and Axe J D 1986 *Phys. Rev.* B **33** 4793
[25] Jorgensen J-E, Staun Olsen J and Gerward L 2000 *J. Appl. Crystallogr.* **33** 276
[26] Ross N L 2000 *Reviews in Mineralogy* vol 41, ed R M Hazen and R T Downs (Washington, DC: The Mineralogical Society of America) ch9
[27] Haines J, Leger J M and Schulte O 1996 *Science* **271** 629